ELSEVIER

Journal of Medical Imaging and Radiation Sciences 45 (2014) 131-136

Journal of Medical Imaging and Radiation Sciences

Journal de l'imagerie médicale et des sciences de la radiation

www.elsevier.com/locate/jmir

Review Article

Model-based Iterative Reconstruction: A Promising Algorithm for Today's Computed Tomography Imaging

Lu Liu, Honours BSc*

Medical Imaging Department, St Michael's Hospital, Toronto, Ontario, Canada

ABSTRACT

Because of its fast image acquisition and the rich diagnostic information it provides, computed tomography (CT) has gradually become a popular imaging modality among clinicians. Because CT scanners emit x-rays, the increased use of CT in clinical applications inevitably leads to increased medical radiation dose to the population. Because of the well-known cancer-inducing effects of high dose x-ray radiation, this increased dose has caused concerns among policy makers and general public that CT patients may be at a higher risk of developing cancer. Over the years, CT manufacturers have developed a variety of strategies to address this issue, the latest being a model-based iterative reconstruction (MBIR) algorithm. MBIR is an advanced CT algorithm that incorporates modeling of several key parameters that were omitted in earlier algorithms to reduce computational requirement and speed up scans. This review article examines the latest literature in the clinical CT field and discusses the general principles of MBIR, its dose and noise reduction potentials, its imaging characteristics, and its limitations. MBIR algorithm and its application in today's CT imaging will greatly reduce the radiation dose to patients and improve image quality for clinicians.

RÉSUMÉ

En raison de la rapidité de l'acquisition de l'image et de la richesse de l'information diagnostique qu'elle offre, la tomographie par ordinateur a rapidement gagné en popularité chez les cliniciens. Puisque les appareils de tomographie émettent des rayons X, leur utilisation croissante dans les applications cliniques conduit inévitablement à une augmentation de la dose de radiation médicale dans la population. En raison des effets cancérigènes bien connus des doses élevées de rayons X, cette dose accrue a soulevé des craintes chez les décideurs et le grand public du fait que les patients soumis à la tomographie par ordinateur puissent présenter un risque plus élevé de souffrir d' un cancer. Au fil des années, les fabricants d'appareils de tomographie par ordinateur ont élaboré différentes stratégies pour aborder cet enjeu, le plus récent étant un algorithme de reconstruction itérative basée sur un modèle (model-based iterative reconstruction - MBIR). Le MBIR est un algorithme avancé de tomographie par ordinateur qui intègre la modélisation de plusieurs paramètres clés omis dans les algorithmes précédents afin de diminuer les exigences de calcul et accélérer le balayage. Cet article recense les plus récents articles publiés dans le domaine de la tomographie clinique et aborde des principes généraux du MBIR, de son potentiel de réduction de la dose et du bruit, de ses caractéristiques d'image et de ses limites. L'algorithme MBIR et son application en imagerie tomographique permettra de diminuer fortement la dose de rayonnement pour les patients et d'améliorer la qualité des images pour les cliniciens.

Keywords: MBIR; model-based iterative reconstruction; CT; computed tomography; radiation dose

Introduction

In 2006, 67 million computed tomography (CT) examinations were performed in the United States alone [1]. The result is an increase of medical radiation dose received as a percentage of the total radiation exposure from 15% in the early 1980s to almost 50% in 2006 [1]. Based on a model known as Biological Effects of Ionizing Radiation [2], Berrington de Gonzalez et al [3] predicted that 29,000 future cancers in the United States will be caused by CT scans performed in the year 2007 alone. Echoing this sentiment, Brenner and Hall [4] estimated that 1%–2% of all cancers in America are caused by CT examinations. In the area of pediatric CT, Pearce et al [5] reported that the risk of leukaemia and brain cancer tripled in children after receiving cumulative doses of about 50 and 60 mGy, respectively.

Because of these concerns associated with ionizing radiation exposure, several dose reduction methods have already been developed by CT manufacturers. The popular techniques that are currently in clinical use include dual-source CT scanners, adaptive noise reduction filters, tube current

The author(s) have no financial disclosures or conflicts of interest to declare.

* Corresponding author: Lu Liu, Honours BSc, Medical Imaging Department, St Michael's Hospital, 30 Bond Street, Toronto, Ontario, Canada M5B 1W8.

E-mail address: liulu@smh.ca

1939-8654
http://dx.doi.org/10.1016/j.jmir.2014.02.002

modulation, and prospective cardiac electrocardiography (ECG) modulation, among others [6]. More recently, the focus of CT dose reduction has been shifted toward iterative reconstruction (IR) algorithms, a new frontier aimed at further reducing the radiation exposure received by patients.

Traditionally, CT images have been produced using analytical reconstruction algorithms such as filtered back projection (FBP) or convoluted back projection instead of IR algorithms because of their simple mathematical computation requirement. Most techniques involving these analytical algorithms neglect the cone-beam geometry of the measured data and depend on false assumptions, which compromise the truthfulness of output images. For example, in FBP and convoluted back projection algorithms, the x-ray source and the individual cell on the detector in a CT scanner are considered infinitely small. Each voxel also has no shape or size. To construct high-quality images, IR algorithms have been used to address some of the weaknesses associated with traditional algorithms. Over the past few years, several IR algorithms have emerged in clinical CT applications. A list of these statistical and model-based IR algorithms can be found in Table 1.

Iterative Reconstruction (IR)

Unlike analytical reconstruction that uses simple mathematical assumptions of a CT imaging system, statistical IR is based on the statistics of random fluctuations in sinogram measurements, also known as the two-dimensional array of raw data containing CT projections [7]. Instead of manipulating data to conform to analytical reconstruction models, statistical and model-based methods try to incorporate a data obtaining, comparing, and updating cycle into the reconstruction process that improves the diagnostic accuracy of the output CT images. There are three major components of an IR algorithm. First, artificial object data from estimation or a standard volume of a similar object are created. Second, these estimated raw data are compared with the real measured data from the imaging system. Third, the difference between these two data sets is projected back to the estimation step for future correction. This entire cycle continues until the difference between the estimated and measured data is within an acceptable range. An example of a statistical IR algorithm, sometimes known as a hybrid IR algorithm because of its ability to blend with FBP, is called adaptive statistical iterative reconstruction (ASIR). It models photons and electric noise in the CT system, and it is not computationally expensive or time-consuming to

Table 1
A List of Statistical and Model-based Iterative Reconstruction Algorithms Developed by Major Computed Tomography Manufacturers Listed in Alphabetical Order

Manufacturer	Statistical IR	Model-based IR
General Electric	ASiR	Veo
Philips	iDose	IMR
Siemens	IRIS	SAFIRE
Toshiba	AIDR 3D (integrated)	AIDR 3D (integrated)

IR, iterative reconstruction.

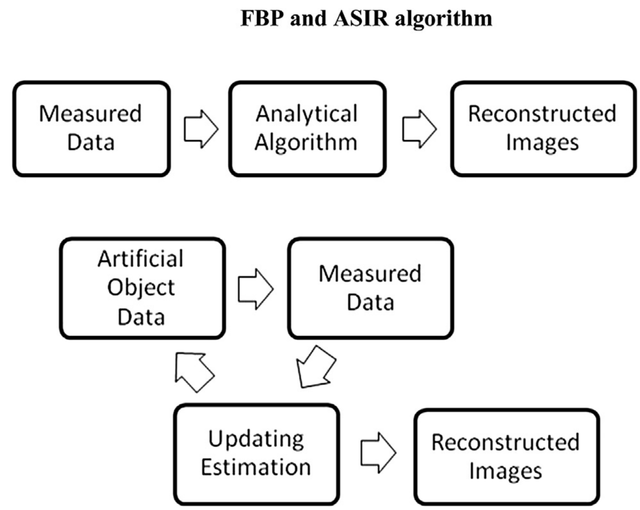

Figure 1. The basic workflow of an FBP (top) and ASIR algorithm (bottom).

perform clinically on today's computer system [8]. The basic workflow for reconstructing CT images using either an FBP or an ASIR algorithm is shown in Figure 1.

More recently, model-based iterative reconstruction (MBIR), also known as pure IR algorithm, has been shown to significantly improve image quality while reducing noise and artifacts in multislice CT scans during initial tests [9, 10]. In MBIR, images are reconstructed by minimizing the objective function incorporated with an accurate system model, a statistical noise model, and a prior model [11]. The system model deals with the nonlinear, polychromatic nature of x-ray tubes by modeling the photons in the measured data set. The statistical noise model takes into consideration the size of an x-ray tube focal spot and the three-dimensional shape of detectors. The prior model is a regularization algorithm that corrects unrealistic situations during reconstruction to speed up the process. A basic workflow of an MBIR algorithm is summarized in Figure 2.

Dose Reduction and Image Characterization in CT Applications

All literature surveyed in this review conducted their studies in a typical clinical setting, with eligible patients

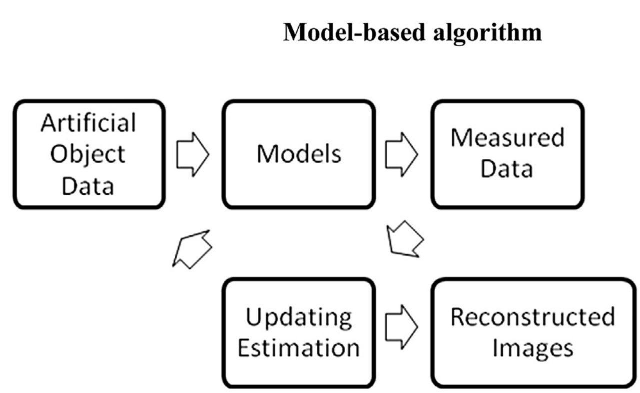

Figure 2. The basic workflow of an MBIR algorithm.

Table 2
A Summary of the General Patient Characterizations and Computed Tomography Parameters Used in the Literature Surveyed

	Sample size	Age (y)/BMI (kg/m^2)/Weight (kg)	Scanner Type	Contrast Enhanced	Slice Thickness (mm)
Chest					
Katsura et al (2012)	100	65.6/NA/58	Helical, 64-slice	No	0.625
Mieville et al (2012)	20	7–18/NA/NA	Helical, 64-slice	No	0.625, 1.25, & 1.41
Neroladaki et al (2012)	42	19–80/Male = 22.8, female = 25.8/NA	Helical, 64-slice	No	0.625
Abdomen					
Deak et al (2013)	22	56.1/NA/79.1	Helical, 64-slice	Yes	0.625/interval = 5
Pickhardt et al (2013)	45	57.9/28.5/NA	Helical, 64-slice	Yes = 21, No = 24	2.5/interval = 1.25
Singh et al (2012)	10	59.9/NA/87.8	Helical, 64-slice	Yes	5/interval = 5
CTA					
Ebersberger et al (2012)	29	67.6/29/NA	Helical, 128-slice	Yes	0.75/interval = 0.4
Tricarico et al (2012)	40	4.6/NA/NA	NA	Yes	1/interval = 0.6
Winklehner et al (2011)	25	70.7/26.9/80.9	Helical, 128-slice	Yes	2/interval = 1.6

BMI, body mass index; NA, not applicable.
Age, BMI, and weight values are the averages of all patients in each corresponding study. Slice thickness refers to the reconstructed slice thickness.

undergoing scans in a consecutive manner. A summary of the patient characterizations and CT scan parameters found in the literature is listed in Table 2. To quantify the radiation dose received by patients, the majority of the studies reviewed first obtained the dose length product through direct measurement of CT dose index ($CTDI_{vol}$) using phantoms. The researchers were then able to convert the DLP into the effective dose with Monte Carlo simulations as estimation of radiation for the full body of a patient [12]. Those studies evaluating the differences in reconstructed CT images with FBP, ASIR, and MBIR predominantly examined both objective and subjective image quality. Objective image quality is measured directly from CT numbers and image noise, whereas subjective image quality involves radiologists independently grading CT images in terms of diagnostic quality. Figures 3 and 4 summarize the dose and quantitative noise reduction observed in the literature surveyed, respectively. It appears that both dose and noise reduction potentials are the greatest in studies performed on chest CT scans, with the highest reported being 98% and 79%, respectively. In comparison, these potentials are less pronounced in abdominal CT and CT angiography (CTA) studies.

Chest

In a study involving 100 adults undergoing noncontrast chest CT scans by Katsura et al [8], the authors reported a mean dose of 1.13 mSv using a low-dose protocol, an almost 80% dose reduction when compared with a reference CT

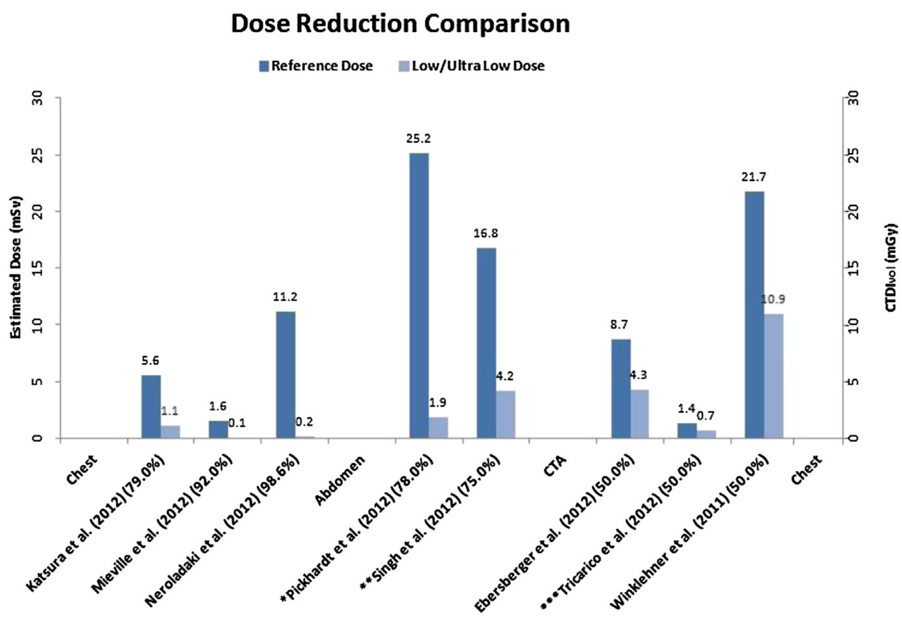

Figure 3. A compilation of dose reduction potential reported in the literature surveyed. The percentages in brackets after each article represent the dose reduction reported by authors. The values were calculated by comparing the lowest-dose protocol with that of the reference protocol. All values were rounded up to one decimal place. Standard deviations from the literature were omitted. The values on top of each column represent the estimated patient dose (primary y-axis) except in the study by **Singh et al, in which they represent $CTDI_{vol}$ (secondary y-axis). *Doses in this study were the averages of combined enhanced and nonenhanced cases. ***For graphing purpose, only the average doses reported from ECG-gated patients were used.

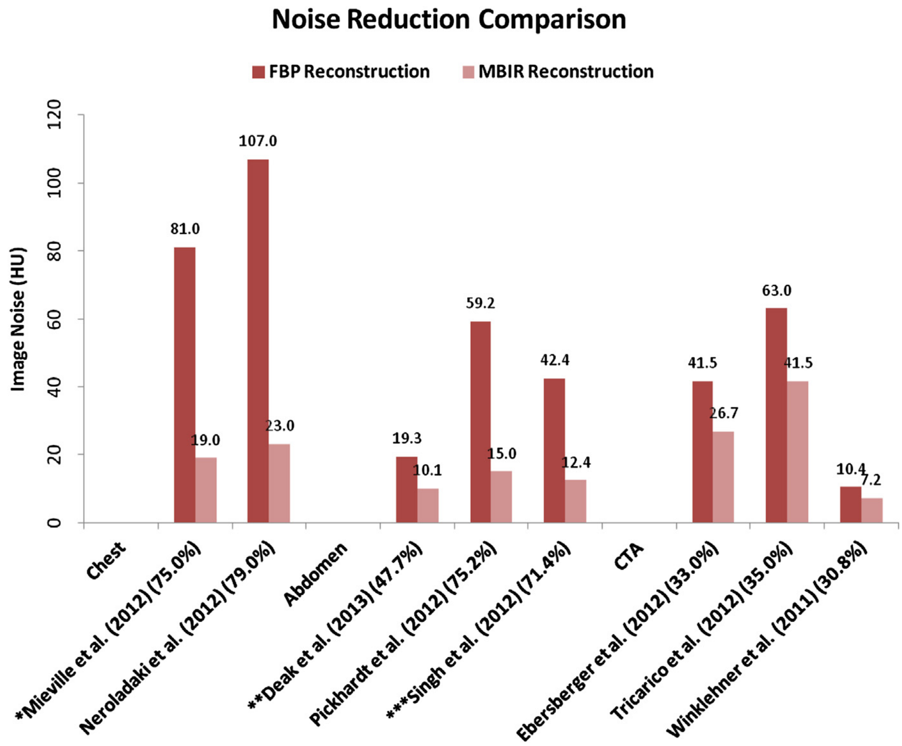

Figure 4. A compilation of noise reduction potential reported by literature surveyed. The percentages in brackets after each article represent noise reduction reported by authors. This was calculated by comparing the objective noise measured in images reconstructed with MBIR with that of the FBP using the lowest-dose protocol. The values on top of each column were the reported mean image noise. All values were rounded up to one decimal place. Standard deviations from the literature are omitted. *Values used for graphing purpose were from axial slices. In articles with ** and ***, the image noise values represent noise in the liver in axial slices.

dose of 5.6 mSv. More excitingly, Mieville et al [13] and Neroladaki et al [14] reported a 92% reduction and an impressive 98.6% reduction for the ultra–low-dose acquisition protocols, respectively. Mieville et al [13] examined 20 pediatric patients receiving unenhanced CT scans and reported 1.6 mSv for the standard CT protocol and only 0.11 mSv for the ultra–low-dose protocol. Neroladaki et al [14] reported a dose as low as 0.16 mSv for 42 unenhanced CT chest scans in adult patients using the minimal dose protocol. The resulting calculated effective radiation dose received under these scans was approaching the radiation dose of roughly 0.05–0.24 mSv, as delivered by a posteroanterior (PA) and lateral chest radiography [15]. However, as noted by Katsura et al [8], the dose reduction effect is reduced in patients with a higher body mass index (BMI) compared with patients with a lower BMI.

Low-dose MBIR images were reported to have significantly less streak artifacts in the lung parenchyma than low-dose ASIR and standard-dose ASIR, whereas the objective noise was higher with MBIR than standard-dose ASIR in the descending aorta [8]. Neroladaki et al [14] reported image noise reduced statistically significantly from 107 Hounsfield Unit (HU) to 23 HU, resulting in a reduction of 79% in scans reconstructed by MBIR algorithm than with FBP. This observation is in agreement with a roughly 75% reduction of noise from 81 HU to 19 HU in pediatric chest CT scans performed by Mieville et al [13] when comparing images reconstructed using MBIR and FBP algorithms with the ultra–low-dose protocol. Most images obtained from low-dose ASIR were graded by radiologists as "diagnostically unacceptable," whereas MBIR images were "fully acceptable" or "probably acceptable" [8]. Although not significant, MBIR allowed better detection of micronodules and some subtle pericardial effusions when acquired with the ultra–low-dose protocol [14].

Abdomen

In one of the first clinical studies on abdominal CT examinations using ASIR, MBIR, and conventional FBP reconstructions, Singh et al [16] reported the possibility of reducing radiation dose by 75%, from a $CTDI_{vol}$ of 16.8 mGy (200-mA protocol) to 4.2 mGy (50-mA protocol) for patients weighing less than 109 kg in a group of 10 adults undergoing contrast-enhanced scans. Similarly, when comparing the effective radiation dose from the ultra–low-dose protocol with that of the standard protocol, Pickhardt et al [17] reported a mean dose reduction of 78% in 45 adult patients, of which 21 patients received contrast-enhanced abdominal CT scans and the other 24 patients had noncontrast scans.

Singh et al [16] reported two- to three-fold lower image noise in 50-mA MBIR compared with 50-mA ASIR, 50-mA FBP, and 200-mA FBP. The finding is again echoed by Pickhardt et al [17], who observed significantly lower mean image noise for MBIR (14.7 HU) than standard-dose FBP (28.9 HU), low-dose FBP (59.2 HU), and ASIR (45.6 HU). Not surprisingly, Deak et al [18] noted 18%–47% lower objective noise in images reconstructed with MBIR than it was for ASIR, which, in turn, was 14%–68% lower than the FBP algorithm. MBIR was also observed to exhibit a major subjective image quality improvement over ASIR, which was again slightly superior compared with images reconstructed with FBP [17, 18]. However, the MBIR was graded slightly lower overall by radiologists when compared with standard-dose FBP [17]. Nevertheless, MBIR was superior to ASIR and FBP at detecting lesions at 50 mA and FBP at 200 mA in all but two patients with higher body weight and larger transverse diameters [16]. Interestingly, Pickhardt et al [17] also found low-dose MBIR permitted significantly more detection of noncalcified focal lesions than low-dose FBP and ASIR, but lower than that detected by standard-dose FBP. In addition, MBIR significantly reduced photon starvation and beam-hardening artifacts in critical anatomic locations including spine and pelvis [18]. On the other hand, the pure IR algorithm did show a subtle staircase effect on cortical bony interfaces and minor bordering blacked-out artifacts solely on the interfaces between skin and air [18].

CT Angiography (CTA)

Two major differences are noted between CTA studies and the chest and abdominal studies mentioned earlier. First of all, all three CTA studies decided to use a predetermined standard-dose and half-dose protocols for their comparison studies. Therefore, the dose reduction numbers reported by these groups are more arbitrary than chest and abdominal studies. Second, the three CTA studies were performed using 128-slice CT scanners as opposed to 64-slice scanners in the chest and abdominal studies. In a neonatal and pediatric CTA study of 40 children, the low-dose protocol was able to deliver an estimated effective dose of 0.68 mSv in an ECG-gated scenario compared with about twice as much radiation dose from a standard protocol [19]. Tricarico et al [19] also reported a lower average dose from 21 non–ECG-gated CTA patients, but essentially the same magnitude of dose reduction as in 19 ECG-gated patients. A 50% dose reduction was achieved by Winklehner et al [20] in their clinical evaluation of 25 adult patients as well. Similarly, although not significant, image quality of half-dose MBIR from a study by Ebersberger et al [21] was still higher than full-dose FBP, suggesting at least a 50% dose reduction using the lower-dose protocol reconstructed with MBIR algorithm compared with FBP.

Overall image quality was again reported to be significantly better with the MBIR algorithm than AISR or FBP algorithms in cardiac CT scanning [22]. Subjective noise in images reconstructed with MBIR was significantly lower than ASIR, which was in turn significantly lower than FBP [22]. Furthermore, sharpness was also improved in MBIR over ASIR, but no significant difference was observed between ASIR and FBP [22]. Quantitative image analysis also showed the MBIR algorithm increased contrast-to-noise ratio by 51%–69% and decreased image noise by 30%–36% when compared with the other two algorithms [22]. In patients with coronary artery stents, the signal-to-noise ratio was significantly better in both standard- and half-dose MBIR reconstructions compared with those reconstructed with either the standard- or half-dose FBP algorithm [21]. Similar observations regarding improved contrast-to-noise and signal-to-noise ratios were made by Tricarico et al [19] when they compared images obtained with half-dose MBIR with that of full-dose and half-dose FBP. The stent-lumen attenuation increase ratio, which determines the effect from high attenuating stents, was also significantly lower in MBIR reconstructions compared with FBP, with the exception that half-dose MBIR did not vary from full-dose FBP [21]. However, Scheffel et al [22] reported no difference in detecting calcifications, and all three algorithms showed a similar level of blooming artifact, which could adversely affect luminal visualization.

Discussion

MBIR algorithm is generally superior to FBP and ASIR in areas of radiation dose and image quality. However, issues surrounding MBIR will need to be addressed before it is to completely replace the other reconstruction algorithms in CT imaging. Low-dose MBIR images were often associated with motion artifacts and a blotchy, pixelated appearance, affecting the visualization of small structures [8, 13]. However, Mieville et al [13] noted an improvement for small structures in the coronal plane compared with the axial plane. As for larger anatomic structures, the authors reported a change of image texture between images reconstructed with MBIR and those with FBP [13]. This new appearance of certain structures will require some time for the radiologic community to adapt in order to achieve more accurate clinical interpretation. Incidentally, similar appearance was also reported in earlier studies evaluating the ASIR technique [23, 24]. Therefore, the cause of this blotchy appearance observed in images reconstructed with MBIR might be linked to software, and it may be eventually overcome by the future improvement of the algorithm itself. Bronchiectasis and architectural distortion were described on ultra–low-dose CT scans reconstructed with MBIR [14]. There was also a possibility that CT images reconstructed with MBIR showed micronodules that did not exist, leading to false-positive results [14]. Although MBIR is excellent at reducing the radiation dose delivered to patients, Singh et al [16] found the diagnostic confidence and subjective image quality in patients over 109 kg were suboptimal during low-dose scans. This suggests that MBIR algorithm may need further updating to enhance the benefits for patients with a higher BMI. Aside from image quality, one of the biggest drawbacks of the MBIR algorithm is the time it requires to reconstruct the raw CT data. An initial study indicated that up to 3 hours of reconstruction time may be needed for the MBIR algorithm depending on patients' size and display field of view [16]. A more recent study performed by Vardhanabhuti et al [25] reported a processing time of approximately 45 minutes per series. In comparison, FBP and ASIR algorithms take only a few seconds to complete. Although the MBIR reconstruction time may be acceptable in nonemergency situations, it does pose as a weakness when a patient's condition requires immediate diagnosis. Nevertheless, with the continued computer hardware improvement and software optimization, the use of the MBIR algorithm in an emergency setting can still be achieved in the future.

Conclusion

The latest studies examined in this review have overwhelmingly shown that the model-based algorithm has great potential in reducing the radiation dose in modern CT scans when compared with the traditional FBP algorithm. In addition to dose reduction, MBIR overwhelmingly decreases image noise, improves spatial and contrast resolution, and reduces some artifacts compared with both the ASIR and FBP algorithms. However, as a novel IR algorithm, MBIR does have limitations that need to be addressed. Aspects of the image characteristics such as image texture and certain artifacts can adversely affect diagnostic confidence. It is also computationally expensive, and it requires a high level of optimization to achieve its intended performance. A diagnostically accurate image obtained with a minimal radiation dose to the patient will be crucial in serving the evermore demanding nature of today's CT applications.

Acknowledgements

The author acknowledges Steves Touliopoulos, MRT(R), Rory Stamina, MRT(R), and the rest of the Medical Imaging Department of Toronto's St. Michael's Hospital for their inspiration and support.

References

[1] National Council on Radiation Protection and Measurements (NCRP). Ionizing radiation exposure of the population of the United States. NCRP Report No. 160, 2007. Available at: http://www.ncrponline.org/Publications/Press_Releases/160press.html. Accessed January 30, 2013.

[2] National Research Council (NRC), Committee to Assess Health Risks from Exposure to Low Levels of Ionizing Radiation (2006). Health risks from exposure to low levels of ionizing radiation: BEIR VII–phase 2. Washington, DC: National Academies Press.

[3] Berrington de Gonzalez, A., Mahesh, M., & Kim, K. P., et al. (2009). Projected cancer risks from computed tomographic scans performed in the United States in 2007. *Arch Intern Med* 169, 2071–2077.

[4] Brenner, D. J., & Hall, E. J. (2007). Computed tomography—an increasing source of radiation exposure. *N Engl J Med* 357, 2277–2284.

[5] Pearce, M. S., Salotti, J. A., & Little, M. P., et al. (2012). Radiation exposure from CT scans in childhood and subsequent risk of leukaemia and brain tumours: a retrospective cohort study. *Lancet* 380, 499–505.

[6] Gunn, M. L., & Kohr, J. R. (2009). State of the art: technologies for computed tomography dose reduction. *Emerg Radiol* 17, 209–218.

[7] Thibault, J. B., Sauer, K. D., Bouman, C. A., & Hsieh, J. (2007). A three-dimensional statistical approach to improved image quality for multislice helical CT. *Med Phys* 34, 4526–4544.

[8] Katsura, M., Matsuda, I., & Akahane, M., et al. (2012). Model-based iterative reconstruction technique for radiation dose reduction in chest CT: comparison with the adaptive statistical iterative reconstruction technique. *Eur Radiol* 22, 1613–1623.

[9] Ziegler, A., Kohler, H., & Proksa, R. (2007). Noise and resolution in images reconstructed with FBP and OSC algorithms for CT. *Med Phys* 34, 585–598.

[10] Wang, G., Yu, H., & De Man, B. (2008). An outlook on X-ray CT research and development. *Med Phys* 55, 1051–1064.

[11] Yu, Z., Thibault, J., Bouman, C. A., Sauer, K. D., & Hsieh, J. (2011). Fast model-based X-ray CT reconstruction using spatially nonhomogeneous ICD optimization. *IEEE Trans Image Process* 20, 161–175.

[12] Deak, P. D., Smal, Y., & Kalender, W. A. (2010). Multisection CT protocols: sex- and age-specific conversion factors used to determine effective dose from dose-length product. *Radiology* 257, 158–166.

[13] Mieville, F. A., Berteloot, L., & Grandjean, A., et al. (2013). Model-based iterative reconstruction in pediatric chest CT: assessment of image quality in a prospective study of children with cystic fibrosis. *Pediatr Radiol* 43, 558–567.

[14] Neroladaki, A., Botsikas, D., Boudabbous, S., Becker, C. D., & Montet, X. (2012). Computed tomography of the chest with model-based iterative reconstruction using a radiation exposure similar to chest X-ray examination: preliminary observations. *Eur Radiol* 23, 360–366.

[15] Huda, W., Nickoloff, E. L., & Boone, J. M. (2008). Overview of patient dosimetry in diagnostic radiology in the USA for the past 50 years. *Med Phys* 35, 5713–5728.

[16] Singh, S., Kalra, M. K., & Do, S., et al. (2012). Comparison of hybrid and pure iterative reconstruction techniques with conventional filtered back projection: dose reduction potential in the abdomen. *J Comput Assist Tomogr* 36, 347–353.

[17] Pickhardt, P. J., Lubner, M. G., & Kim, D. H., et al. (2012). Abdominal CT with model-based iterative reconstruction (MBIR): initial results of a prospective trial comparing ultralow-dose with standard-dose imaging. *AJR Am J Roentogenol* 199, 1266–1274.

[18] Deak, Z., Grimm, J. M., & Treitl, M., et al. (2013). Filtered back projection, adaptive statistical iterative reconstruction, and a model-based iterative reconstruction in abdominal CT: an experimental clinical study. *Radiology* 266, 197–206.

[19] Tricarico, F., Hlavacek, A. M., & Schoepf, U. J., et al. (2013). Cardiovascular CT angiography in neonates and children: Image quality and potential for radiation dose reduction with iterative image reconstruction techniques. *Eur Radiol* 23, 1306–1315.

[20] Winklehner, A., Karlo, C., & Puippe, G., et al. (2011). Raw data-based iterative reconstruction in body CTA: evaluation of radiation dose saving potential. *Eur Radiol* 21, 2521–2526.

[21] Ebersberger, U., Tricarico, F., & Schoepf, U. J., et al. (2012). CT evaluation of coronary artery stents with iterative image reconstruction: improvements in image quality and potential for radiation dose reduction. *Eur Radiol* 23, 125–132.

[22] Scheffel, H., Stolzmann, P., & Schlett, C. L., et al. (2011). Coronary artery plaques: cardiac CT with model-based and adaptive-statistical iterative reconstruction technique. *Eur J Radiol* 81, 363–369.

[23] Prakash, P., Kalra, M. K., & Digumarthy, S. R., et al. (2010). Radiation dose reduction with chest computed tomography using adaptive statistical iterative reconstruction technique: initial experience. *J Comput Assist Tomogr* 34, 40–45.

[24] Sagara, Y., Hara, A. K., & Pavlicek, W., et al. (2010). Abdominal CT comparison of low-dose CT with adaptive statistical iterative reconstruction and routine-dose CT with filtered back projection in 53 patients. *AJR Am J Roentgenol* 195, 713–719.

[25] Vardhanabhuti, V., Loader, R. J., Mitchell, G. R., Riordan, R. D., & Roobotom, C. A. (2013). Image quality assessment of standard- and low-dose chest CT using filtered back projection, adaptive statistical iterative reconstruction, and novel model-based iterative reconstruction algorithms. *AJR Am J Roentgenol* 200, 545–552.